

KINETICS OF HYDROGEN CONSUMPTION DURING CATALYTIC HYDRODESULPHURIZATION OF A RESIDUE IN A TRICKLE-BED REACTOR

NICKOS PAPAYANNAKOS AND GEORGE GEORGIU

Laboratory of Chemical Process Engineering,
National Technical University of Athens,
106 82 Athens, Greece

Key Words: Chemical Reaction, Kinetics, Hydrogen Consumption, Catalytic Hydrodesulphurization, Effective Diffusivity

A kinetic model for hydrogen consumption during catalytic residue hydrodesulphurization, is presented. The intrinsic reaction rates are described by use of a second-order kinetic equation. The intraparticle diffusional effects are discussed by means of the effective diffusivity. Kinetic experiments were carried out in an isothermal trickle-bed reactor, in which two commercial Co-Mo/Al₂O₃ catalysts were used in a temperature range of 350–430°C, a liquid hourly space velocity ranging from 0.25 to 3 h⁻¹, and a constant pressure of 50 × 10⁵ Pa. The remaining catalyst activity varied between 1.0 and 0.2. Crushed particles and cylindrical extrudates—for each type of catalyst—were used in experimentation. The atmospheric residue of Greek petroleum deposits in the Aegean Sea served as feedstock. Specific rate constants, activation energies and effective diffusivities were determined. Hydrogen consumption increased as either the remaining activity of the catalyst, the reactor temperature or the catalyst size decreased.

Introduction

The direct catalytic hydrodesulphurization process is employed to reduce the sulphur content of residues and improve their quality. Hydrogen consumption during the catalytic hydrodesulphurization constitutes the largest element of the operating cost. Only the cost of the catalyst used may approach that of the hydrogen consumed, if the feeds contain large amounts of metals.⁷⁾ The most precise knowledge of the hydrogen consumption is, therefore, of primary importance.

The most interesting reactions consuming hydrogen during residue catalytic hydrodesulphurization are: (1) hydrodesulphurization and hydrodenitrogenation reactions, which consume one molecule of hydrogen for each carbon-sulphur or carbon-nitrogen bond cleavage; (2) hydrocracking reactions, which consume one molecule of hydrogen for each carbon-carbon bond cleavage; and (3) hydrogenation reactions, which consume one molecule of hydrogen for the saturation of each double bond and two molecules of hydrogen for the saturation of each triple bond. These reactions occur in parallel and the observed hydrogen consumption rates are the summation of the rates of the hydrogen consumed in each reaction type. The total hydrogen reaction

rate, therefore, is affected by all parameters affecting each reaction separately.

The data presented to date in the literature allow only a rough correlation between the hydrogen consumed during hydrodesulphurization and the degree of desulphurization^{1,2,7,8,11,12)} because there is as yet no model relating the process conditions and the performance of the catalyst used with the hydrogen consumption rates.

In this paper, a simple kinetic model for hydrogen consumption during catalytic hydrodesulphurization is presented, including the effects of reactor conditions and catalyst type, size and age. Kinetic data for hydrogen consumption during catalytic hydrodesulphurization of the atmospheric residue obtained from Greek petroleum deposits in the Aegean Sea are presented and the catalyst selectivity is discussed.

1. Experimental

Figure 1 shows schematically the experimental apparatus used in this study. The inside diameter of the reactor was 2.54 × 10⁻² m. The properties and dimensions of the four catalyst beds employed are shown in Table 1. Entrance and exit flow maldistributions were avoided by using inert particles at both ends of the catalyst beds.⁶⁾ A thermowell was inserted through the catalyst beds, having five thermocouples located along its length to monitor the

Received March 5, 1987. Correspondence concerning this article should be addressed to N. Papayannakos.

Table 1. Catalyst bed characteristics

Characteristic	Catalyst bed			
	HT 400E	HT 400E	G-51	G-51
Catalyst used	HT 400E	HT 400E	G-51	G-51
Particle shape	Crushed particles	Cylindrical extrudates	Crushed particles	Cylindrical extrudates
Particle mean diameter, m	0.34×10^{-3}	1.59×10^{-3}	0.34×10^{-3}	3.00×10^{-3}
Catalyst weight, kg	101.9×10^{-3}	121.9×10^{-3}	102.7×10^{-3}	102.4×10^{-3}
Catalyst volume, m ³	139.7×10^{-6}	156.6×10^{-6}	142.2×10^{-6}	152.5×10^{-6}
Catalyst apparent density, kg/m ³	1.30×10^3	1.30×10^3	1.38×10^3	1.38×10^3
Void fraction	0.43	0.40	0.48	0.52

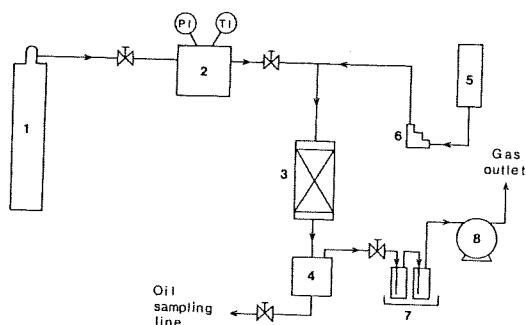


Fig. 1. Schematic diagram of apparatus
1, H₂ cylinder; 2, H₂ accumulator; 3, reactor; 4, phase separator; 5, oil reservoir; 6, oil pump; 7, H₂S absorbers; 8, gas meter.

isothermality of the beds.

The sulphur content of the residue was 5.0 ± 0.2 wt%, the metal (Ni + V) content was less than 20 ppm and the specific gravity 15/4°C of the residue was 1.003. The catalysts used were of the commercial type HT 400E (donated by Harshaw Chemie B.V., De Meern, The Netherlands) and G-51 (donated by Süd-Chemie A.G., Sparte Katalysatoren, München). Pore size distribution measurements indicated that crushed particles had retained the structure of pattern extrudates. The properties of catalysts are shown in **Table 2**. The catalysts were reduced *in situ* before commencing kinetic experiments.⁹⁾

Hydrogen consumption measurements were taken during steady-state reaction conditions. The gas accumulator was filled with hydrogen (up to 100×10^5 Pa) and isolated from the hydrogen cylinder, feeding the reactor at 50×10^5 Pa. Hydrogen inlet flowrates were determined by recording the pressure and temperature of the gas accumulator during timing. The exit hydrogen flowrate was measured by a gas meter after pressure had been reduced to 1×10^5 Pa and was kept at $(1.25 \pm 0.14) \times 10^{-5}$ Nm³/s. The solubility of hydrogen in desulphurized residue at the conditions prevailing in the phase separator and volatile hydrocarbon content in the effluent gas have been taken into account for accurate calculation of hydrogen consumption. The sulphur content in feedstock and desulphurized products were measured by an X-ray analyser.

Table 2. Properties of catalysts

Property	Catalyst	
	A	B
Type	HT 400E	G-51
wt% CoO	3.0	3.5
wt% MoO ₃	15.0	10.0
wt% Al ₂ O ₃	82.0	86.5
Specific surface area S_p , m ² /kg	230×10^3 **	235×10^3 **
Total pore volume V_p , m ³ /kg	0.50×10^{-3} **	0.63×10^{-3} **
Mean pore radius, m	43×10^{-10}	54×10^{-10}

* The mean pore radius was calculated as $2V_p/S_p$.

** Measured.

Standard experiments were carried out to determine the catalyst remaining activity for hydrodesulphurization and hydrogen consumption. It was shown that the remaining activity for hydrodesulphurization was identical, within the experimental error, to the remaining activity for hydrogen consumption.

Application of the criterion given by Satterfield,¹⁰⁾ $(10d_p) R^*(1-\epsilon) < k_{ts} \cdot c^*$, shows that external mass transfer limitations are negligible for both hydrogen consumption and hydrodesulphurization of the oil, across the range of experimental conditions of this work. Contacting effectiveness was found to have values in the range 0.25–0.35 from data given in the literature.^{5,10)}

2. Kinetic Model

The differential mass balance equation of the hydrogen, which reacts with the various organic compounds in the residue as described above, in the tubular reactor according to the isothermal plug-flow model is

$$\eta \xi (1-\epsilon) R dV_R = -Q_L dCH \quad (1)$$

where R is the hydrogen reaction rate, CH stands for the remaining hydrogen demand or, likewise, for the concentration of the bonds which are bound to react with hydrogen at the reaction conditions, expressed in mol H₂ per m³ of the oil. Therefore, the total hydrogen consumption CH_T represents the concentration of all the bonds likely to react with hydro-

gen at the reaction conditions before any treatment occurs.

The observed reaction rate of hydrogen consumption comprises the sum of the reaction rates of hydrogen with the bonds likely to react in oil and can be described by the following kinetic equation:

$$R = k_v(CH)^\alpha \quad (2)$$

where k_v stands for the rate constant and α for the reaction order. This kinetic formula has been successfully used to describe reaction rates in mixtures of compounds with a wide distribution of reactivities, such as hydrodesulphurization of petroleum fractions and residua,^{2,3,9)} catalytic cracking,⁴⁾ etc., though it is meaningless mechanistically. Reaction order α will depend on the concentration and reactivity of the reacting molecules. k_v in Eq. (2) includes the hydrogen partial pressure term ($k_v = k_v^* P_{H_2}^\beta$) because this pressure is considered constant in this work.

In the absence of intraparticle diffusion effects, $\eta = 1$, and after replacing R in Eq. (1) from (2) and integrating the former we can derive the following equation:

$$(CH)^{1-\alpha} - (CH_T)^{1-\alpha} = (\alpha-1)\xi(1-\varepsilon)k_v(V_R/Q_L) \quad (3)$$

When intraparticle diffusional effects are significant, $\eta < 1$, Eq. (1) can be integrated only when the dependence of the effectiveness factor η , on the remaining hydrogen demand of the oil CH , is a known function. Froment and Bishoff⁴⁾ presented a figure which gives a good correlation of the effectiveness factor with the generalized Thiele modulus Φ which, in this case, is represented as:

$$\Phi = \bar{L}_p \sqrt{\frac{(\alpha+1)\xi k_v}{2D_e}(CH)^{\alpha-1}} \quad (4)$$

where D_e is the effective diffusivity in the catalyst pores. An empirical correlation of η and Φ can be used when $2 \leq \alpha \leq 3$, in the following form:

$$\eta = \frac{1}{\sqrt{\Phi^2 + 1}} \quad (5)$$

The mean deviation of the values of η calculated from Eq. (5) is less than 2.4% from those predicted by Froment and Bishoff's correlation in the range $0.99 < \eta < 0.05$.

In replacing η in Eq. (5), in Eq. (1), we proceed to the following form:

$$\int_{CH_T}^{CH} \frac{\sqrt{W(CH)^{\alpha-1} + 1}}{(CH)^\alpha} dCH = -\xi k_v(1-\varepsilon)(V_R/Q_L) \quad (6)$$

where

$$W = (\bar{L}_p)^2 \frac{(\alpha+1)}{2} \xi k_v / D_e \quad (7)$$

Eq. (6) can be solved to give

$$\begin{aligned} & \frac{\sqrt{W(CH)^{\alpha-1} + 1}}{W(CH)^{\alpha-1}} + \ln \frac{\sqrt{W(CH)^{\alpha-1} + 1} + 1}{\sqrt{W(CH)^{\alpha-1}}} \\ & - \frac{\sqrt{W(CH_T)^{\alpha-1} + 1}}{W(CH_T)^{\alpha-1}} - \ln \frac{\sqrt{W(CH_T)^{\alpha-1} + 1} + 1}{\sqrt{W(CH_T)^{\alpha-1}}} \\ & = \frac{\xi k_v(1-\varepsilon)(\alpha-1)}{W} \left(\frac{V_R}{Q_L} \right) \end{aligned} \quad (8)$$

The remaining hydrogen demand CH indicates the difference between the total hydrogen consumption CH_T and the experimentally measured hydrogen consumption CON .

3. Discussion of Results

The reaction order and the total hydrogen consumption were determined by regression analysis of the experimental data in the absence of diffusional effects in the catalyst particles ($d_p = 0.34$ mm). The total hydrogen reaction rate was found to be of second order, $\alpha = 2$, while the total hydrogen consumption was determined as $CH_T = 10.7 \times 10^3$ mol H_2/m_{oil}^3 , within the temperature range 350–430°C for both catalyst types.

The predicted value of CH_T from diagrams in the literature,⁷⁾ based on the °API of the residue, is $CH_T = 8.6 \times 10^3$ mol H_2/m_{oil}^3 . Beuther *et al.*²⁾ measured the hydrogen consumption of a vacuum residue resembling in properties the atmospheric residue used in this study as $CON = 11.5 \times 10^3$ mol H_2/m_{oil}^3 for over 99.2% hydrodesulphurization. This value of hydrogen consumption should be very close to the value of the total hydrogen consumption.

For the second-order reaction of hydrogen consumption, Eq. (3) takes the form

$$\frac{1}{\xi} \frac{CON}{(CH_T - CON)CH_T} = (1-\varepsilon)k_v V_R/Q_L \quad (9)$$

The correlation of the experimental data for the calculation of the intrinsic reaction rate constant k_v in the temperature range 350–430°C for catalyst A are presented in Fig. 2.

An Arrhenius plot of the intrinsic rate constants for hydrogen consumption is shown in Fig. 3. The dependence of the hydrodesulphurization intrinsic rate constants on the temperature of the reaction is also presented in the same figure. The reaction order for hydrodesulphurization using catalyst B was found to be 2.5, as for catalyst A,⁹⁾ while the activation energies are the same within the experimental error. Sulphur concentrations at the reactor outlet were

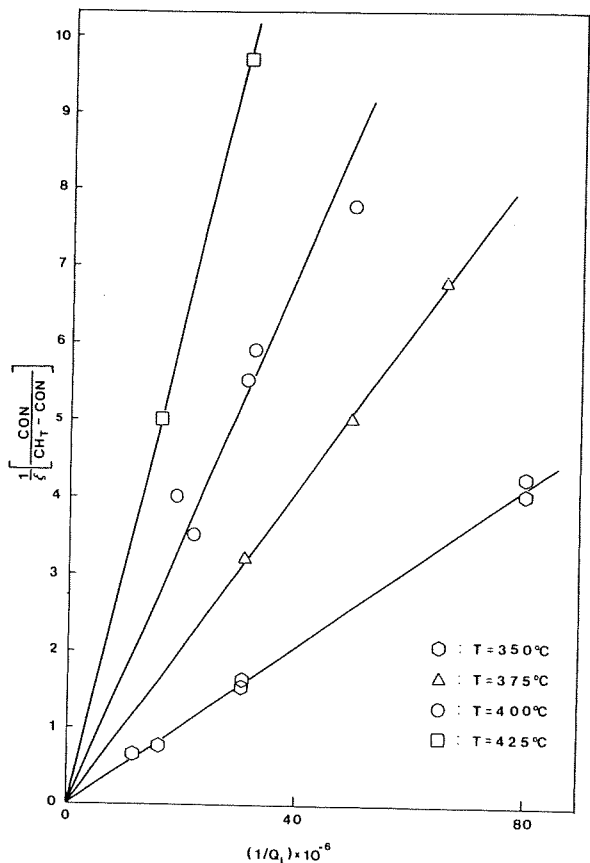


Fig. 2. Second-order kinetics test plot Catalyst A. Catalyst particle size $d_p = 0.34 \times 10^{-3}$ m.

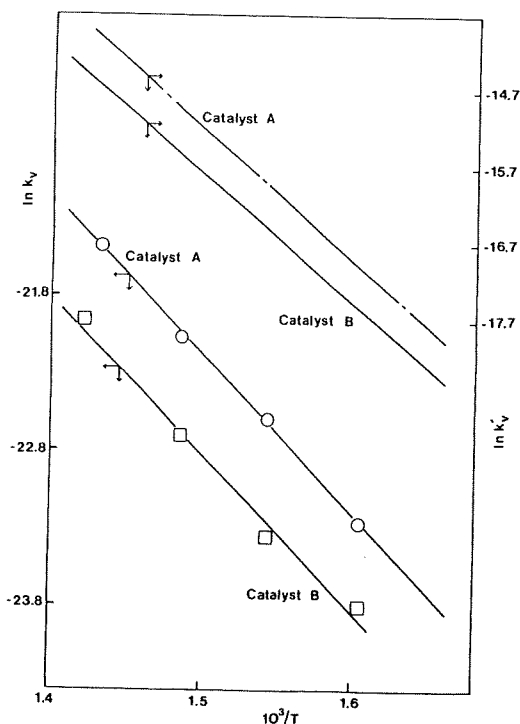


Fig. 3. Arrhenius plot for hydrogen consumption (k_v) and hydrodesulphurization (k'_v) Catalyst particle size $d_p = 0.34 \times 10^{-3}$ m.

calculated according to a plug flow, isothermal model:

$$\int_{S_{in}}^{S_{out}} \frac{1}{\eta} \frac{dS}{S^{2.5}} = -\xi(1-\epsilon)k'_v \frac{V_R}{Q_L} \quad (10)$$

The activation energy for hydrogen consumption is calculated as (86.2 ± 4) kJ/mol H_2 for both types of catalysts and the intrinsic rate constants are calculated as follows:

$$\text{Catalyst A: } k_v = 1.17 \times 10^{-3} \exp(-10,300/T),$$

$$(m_{oil}^3)^2 / \{s(\text{mol } H_2)(m_{cat}^3)\}$$

$$\text{Catalyst B: } k_v = 6.21 \times 10^{-4} \exp(-10,300/T),$$

$$(m_{oil}^3)^2 / \{s(\text{mol } H_2)(m_{cat}^3)\}$$

Intrinsic reaction rates for hydrogen consumption and hydrodesulphurization are lower for catalyst B than for catalyst A. This can be attributed to the different MoO_3 content, since the difference in specific surface area cannot account for the reaction rate differences.

The remaining activity of the catalyst, as a fraction of the initial value, for hydrogen consumption was determined to be the same to that for hydrodesulphurization reactions as discussed in the experimental part and indicated in Table 3 for catalyst A. By using Eq. (8), the effective diffusivity D_e for each experimental run can be calculated. Thus, for commercial extrudates of the catalysts, in the reaction temperature range 350–430°C, the data were satisfactorily correlated by the proposed model, according to Eq. (8), while D_e values were given as follows:

$$\text{Catalyst A: } D_e = (5.1 \pm 1.3) \times 10^{-12} \text{ m}^2/\text{s}$$

$$\text{Catalyst B: } D_e = (1.4 \pm 0.4) \times 10^{-11} \text{ m}^2/\text{s}$$

The effective diffusivities for the hydrodesulphurization were determined as $D_e = (2.5 \pm 1.0) \times 10^{-11} \text{ m}^2/\text{s}$ for the extrudates of catalyst A and $D_e = (7.0 \pm 1.4) \times 10^{-11} \text{ m}^2/\text{s}$ for the extrudates of catalyst B. It is observed that the effective diffusivities of catalyst B are 2.8 times those of catalyst A. This is because pore volume and mean pore diameter of catalyst B were 26% higher than those of catalyst A, as shown in Table 2. The values of the effective diffusivity for hydrogen consumption are lower than those for hydrodesulphurization. This can be attributed to the fact that a certain amount of hydrogen, depending on the severity of the reaction, is consumed for the hydrocracking of the high-molecular weight residual compounds while sulphur is distributed in compounds having molecular weights throughout the whole range of the residual compounds molecular weight. Good agreement between the experimentally determined hydrogen consumption and values predicted by the model was found,

Table 3. Remaining activity of catalyst A for hydrodesulphurization and hydrogen consumption. $d_p = 0.34 \times 10^{-3}$ m, $T = 350^\circ\text{C}$, $Q_L = 3.9 \times 10^{-8}$ m³/s

Time, h	3	15	24	39	55	80	95
Hydrogen consumption, mol H ₂ /m ³ _{oil}	6.6×10^3	6.1×10^3	5.8×10^3	5.3×10^3	4.5×10^3	3.4×10^3	3.0×10^3
Desulphurization, %	75.6	73.4	71.9	67.5	60.3	53.9	50.9
Catalyst remaining activity for hydrogen consumption	1	0.83	0.74	0.61	0.45	0.29	0.24
Catalyst remaining activity for hydrodesulphurization	1	0.86	0.78	0.60	0.41	0.30	0.26

as shown in Figs. 4 and 5.

The influence of catalyst deactivation, catalyst particle size and reaction temperature on the selectivity of the catalyst particles could be very informative regarding catalyst behaviour during the hydrodesulphurization process. Figures 4 and 5 correlate the relative hydrogen consumption with the degree of desulphurization for the two commercial catalyst extrudates at two levels of the remaining activities of the catalyst in the temperature range 350–425°C. It is observed that higher reaction temperatures result in lower hydrogen consumption for any desulphurization level and remaining activity for both types of catalysts. As catalyst remaining activity decreases with time, hydrogen consumption increases, but as the reaction temperature increases, the difference in consumption decreases and at $T = 425^\circ\text{C}$ the consumption values are not significantly different.

Conclusions

The kinetic model developed for hydrogen consumption during catalytic hydrodesulphurization correlated well the experimentally measured hydrogen consumption. The intrinsic activation energy for the hydrogen reaction and consumption was determined as (86.2 ± 4) kJ/mol H₂. Strong pore diffusion limitations were indicated for commercial-size catalyst particles. Decrease of reaction temperature or increase of catalyst deactivation would result in increased hydrogen consumption for a certain degree of desulphurization.

Nomenclature

c^*	= concentration in bulk of oil	[mol/m ³ _{oil}]
CH	= remaining hydrogen demand of oil	[mol H ₂ /m ³ _{oil}]
CH_T	= total hydrogen consumption	[mol H ₂ /m ³ _{oil}]
CON	= hydrogen consumption	[mol H ₂ /m ³ _{oil}]
D_e	= effective diffusivity	[m ² /s]
d_p	= catalyst particle diameter	[m]
k_{1s}	= mass transfer coefficient	[m/s]
k_v	= intrinsic reaction rate constant for hydrogen consumption	$[(\text{m}_{\text{oil}}^3)^2 / ((\text{m}_{\text{cat}}^3) (\text{mol H}_2) (\text{s}))]$
k'_v	= intrinsic reaction constant for hydrodesulphurization	$[(\text{m}_{\text{oil}}^3)^{2.5} / ((\text{m}_{\text{cat}}^3) (\text{mol S})^{1.5} (\text{s}))]$
\bar{L}_p	= catalyst particle volume to external	

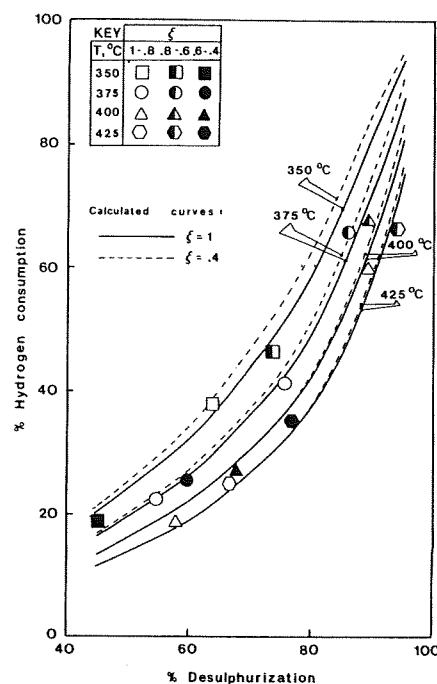


Fig. 4. % Hydrogen consumption ($100 \times CON/CH_T$) vs. % hydrodesulphurization for extrudates of catalyst A

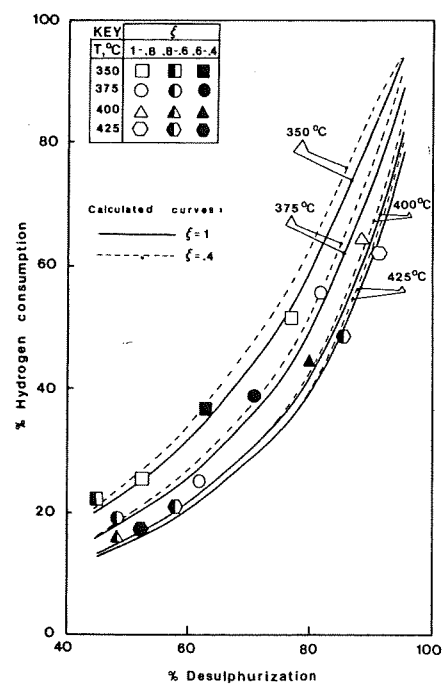


Fig. 5. % Hydrogen consumption ($100 \times CON/CH_T$) vs. % hydrodesulphurization for extrudates of catalyst B

	surface ratio	[m]
Q_L	= oil volumetric flowrate	[m ³ /s]
R	= hydrogen reaction rate	[mol H ₂ /{s(m ³ _{cat})}]
R^*	= reaction rate	[mol/{s(m ³ _{cat})}]
S_{in}, S_{out}	= sulphur concentration in the oil, at inlet and outlet of reactor	[molS/m ³ _{oil}]
T	= temperature	[K]
V_R	= catalyst bed volume	[m ³]
α	= reaction order	[—]
ξ	= catalyst remaining relative activity	[—]
ε	= catalyst bed void fraction	[—]
η	= catalyst effectiveness factor	[—]
Φ	= Thiele modulus	[—]

Literature Cited

- 1) Audibert, F. and J. C. Lavergne: *Chem. Eng. Prog.*, **67**, 71 (1971).
- 2) Beuther, H. and B. K. Schmid: 6th World Petroleum Congress, Section III, p. 297 (1963).
- 3) De Bruijn, A., I. Naka and J. W. M. Sonnemans: *Ind. Eng. Chem. Proc. Des. Dev.*, **20**, 40 (1981).
- 4) Froment, G. F. and K. B. Bischoff: "Chemical Reactor Analysis and Design," John Wiley and Sons, New York (1979).
- 5) Garcia, W. and J. M. Pazos: *Chem. Eng. Sci.*, **37**, 1589 (1982).
- 6) Levenspiel, O.: "Chemical Reaction Engineering," 2nd ed., John Wiley and Sons, New York (1972).
- 7) Nelson, W. L.: O.G.J., Feb. 28, 126 (1977).
- 8) Ohtsuka, T., Y. Hasegawa, M. Koizumi and T. Ono: *Bull. Petrol Inst. Japan*, **9**, 1 (1967).
- 9) Papayannakos, N. and J. Marangozis: *Chem. Eng. Sci.*, **39**, 1051 (1984).
- 10) Satterfield, C. N.: *AIChE J.*, **21**, 209 (1975).
- 11) Takeuchi, C., Y. Fukui, M. Nakamura and Y. Shiroto: *Ind. Eng. Chem. Proc. Des. Dev.*, **22**, 236 (1983).
- 12) Weekman, W.: Proc. 4th Int. Symp. Chem. Reaction Eng., p. 615, DECHEMA, Frankfurt (1976).